

Condition for directly testing scalar modes of gravitational waves by four detectors

Yuki Hagihara, Naoya Era, Daisuke Iikawa, Naohiro Takeda, and Hideki Asada
Graduate School of Science and Technology, Hirosaki University, Aomori 036-8561, Japan
 (Dated: March 13, 2024)

General metric theories in a four-dimensional spacetime allow at most six polarization states (two spin-0, two spin-1 and two spin-2) of gravitational waves (GWs). If a sky location of a GW source with the electromagnetic counterpart satisfies a single equation that we propose in this paper, both the spin-1 modes and spin-2 ones can be eliminated from a certain combination of strain outputs at four ground-based GW interferometers (e.g. a network of aLIGO-Hanford, aLIGO-Livingston, Virgo and KAGRA), where this equation describes curves on the celestial sphere. This means that, if a GW source is found in the curve (or its neighborhood practically), a direct test of scalar (spin-0) modes separately from the other (vector and tensor) modes becomes possible in principle. The possibility of such a direct test is thus higher than an earlier expectation (Hagihara et al. PRD, 100, 064010, 2019), in which they argued that the vector modes could not be completely eliminated. We discuss also that adding the planned LIGO-India detector as a fifth detector will increase the feasibility of scalar polarization tests.

PACS numbers: 04.80.Cc, 04.80.Nn, 04.30.-w

I. INTRODUCTION

The greatest achievement in Einstein's theory of general relativity (GR) is that our spacetime is not a fixed flat background but becomes a dynamical system, and it is described by using a metric in pseudo Riemannian geometry [1, 2]. GR may be conflict with suggestions from quantum physics and string theoretical viewpoints, though GR has passed the parameterized post-Newtonian (PPN) tests over a century and it is consistent also with aLIGO and Virgo observations of gravitational waves (GWs) [3]. The PPN tests are limited within a weak field such as the solar system (or mildly relativistic system such as a binary pulsar). In this sense, GW observations in a strong field must be important for probing new physics beyond GR. General metric theories in a four-dimensional spacetime allow at most six GW polarization states (two spin-0, two spin-1 and two spin-2) [4]. Note that two scalar modes (called Breathing and Longitude modes) are degenerate for interferometers [5]. Hence, we consider a combination of the two scalar modes in this paper.

The first test on the GW polarizations was done for GW150914 [6]. This test is inconclusive, because the number of GR polarizations in GR was equal to the number of aLIGO detectors. The addition of Virgo to the GW detector network allowed for the first informative test of GW polarizations for GW170814. Their analysis shows that the GW data are described better by the pure tensor modes than pure scalar or pure vector modes, with Bayes factors in favor of tensor modes of more than 100 and 200, respectively [7]. A range of tests of GR for GW170817, the first observation of GWs from a binary neutron star inspiral, were done by aLIGO and Virgo [8]. The tests include a test similar to Ref. [7] by performing a Bayesian analysis of the signal properties with the three detector outputs, using the tensor, the vector or the scalar response functions, though the signal-to-noise

ratio in Virgo was significantly lower than those in the two aLIGO detectors. Note that the data stream in Virgo still carries information about the signal. The prospects for polarization tests were discussed (e.g. [9–12]).

KAGRA is expected to soon add to the network of GW detectors [13]. The four noncoaligned GW detectors will allow for better tests of extra GW polarizations and stronger constraints on them. Generally speaking, the number of the detectors including KAGRA is still smaller than the maximum number of the possible polarizations. Hagihara et al. found that there exist particular sky positions that allow a test of vector modes separately from the other modes, because the contributions of possible scalar modes from the GW source in a particular sky direction can be canceled out in a linear combination of the detectors' outputs [14].

Investigating scalar modes is more important than vector modes, because many theories of modified gravity, notably scalar-tensor theories, have attracted a lot of interest so far [15]. Therefore, Hagihara et al. examined whether both vector and tensor modes can be perfectly killed in a sky position [16]. They did not find such particular sky positions. However, there exist some source regions in which the contributions from vector modes are not zero but significantly small with killing tensor modes.

The main purpose of the present paper is to examine whether only the scalar modes can be extracted from a linear combination of the outputs of four detectors. We show that, if a GW source is found in a particular sky region, the scalar modes can be tested separately from the other (vector and tensor) modes in principle.

This paper is organized as follows. In Section II, we discuss how to find a particular linear combination of the detector outputs for perfectly killing both the vector mode and the tensor one. Section III mentions the arrival time difference between detectors. Section IV is devoted to Conclusion.

Throughout this paper, c denotes the speed of light.

Latin indices a, b, \dots run from 1 to 4 corresponding to four detectors. We use the Einstein's summation convention ($A^a B_a = A^1 B_1 + A^2 B_2 + A^3 B_3 + A^4 B_4$). I, J, \dots mean GW polarizations.

II. EXTRACTING ONLY THE SCALAR MODES

A. Basic formulation

Let us imagine four noncoaligned detectors ($a = 1, 2, 3, 4$). As is the case of GW events with an electromagnetic (EM) counterpart such as GW170817 [17], we assume also that, for a given GW source, we know its sky position. By this second assumption, we know exactly how to shift the arrival time of the GW from detector to detector.

A general metric theory in a four-dimensional space-time allows at most six polarizations [4]; h_S for a spin-0 breathing mode, h_L for a spin-0 longitudinal mode, h_V and h_W for two spin-1 modes, h_+ for a spin-2 plus mode and h_\times for a spin-2 cross mode. The antenna pattern function of each detector to these polarization modes is denoted as F_a^I , where $I = S, L, V, W, +, \times$ [18–20]. F_a^I is a function of the GW source direction and the polarization angle. The subscript a of F_a^I for a polarization state means a label in the configuration space of the four detectors but not in the physical spacetime.

The strain output at each detector is a superposition as [5, 18]

$$\begin{aligned} S_a &= F_a^S (h_S - h_L) + F_a^V h_V + F_a^W h_W + F_a^+ h_+ + F_a^\times h_\times \\ &\quad + n_a \\ &= \sum_{I=S}^{\times} F_a^I h_I + n_a, \end{aligned} \quad (1)$$

where n_a denotes a noise.

First, we study how to eliminate three polarization modes from the signal output in Eq. (1). We introduce the Levi-Civita symbol in the detector configuration space ε^{abcd} (a, b, c, d take from 1 to 4), where $\varepsilon^{1234} = 1$, ε^{abcd} is completely antisymmetric, and the superscripts such as $abcd$ are denoting GW detectors. Therefore, ε^{abcd} is independent of coordinate transformations and hence it is a scalar in the physical spacetime.

By noting the complete antisymmetry of ε^{abcd} , one can show $(\varepsilon^{abcd} F_a^W F_b^+ F_c^\times) F_d^W = (\varepsilon^{abcd} F_a^W F_b^+ F_c^\times) F_d^+ = (\varepsilon^{abcd} F_a^W F_b^+ F_c^\times) F_d^\times = 0$. Namely, $\varepsilon^{abcd} F_b^W F_c^+ F_d^\times$ is normal to every of F_a^W , F_a^+ and F_a^\times .

We define a projection operator in a space of the antenna pattern functions. For F_a^I , F_b^J and F_c^K , we define

$$\Pi^{aIJK} \equiv \varepsilon^{abcd} F_b^I F_c^J F_d^K. \quad (2)$$

By using this projection operator, we eliminate three polarizations from the signal output. For $I = W$, $J = +$ and $K = \times$ for example, the projection operator becomes

$\Pi^{aW+\times}$. For this example, h_W , h_+ and h_\times in the strain outputs $\{S_a\}$ are eliminated as

$$\begin{aligned} \Pi^{aW+\times} S_a &= (\varepsilon^{abcd} F_a^S F_b^W F_c^+ F_d^\times) (h_S - h_L) \\ &\quad + (\varepsilon^{abcd} F_a^V F_b^W F_c^+ F_d^\times) h_V + \Pi^{aW+\times} n_a. \end{aligned} \quad (3)$$

We refer to Eq. (3) as a $W + \times$ null stream. By the same way, we can define ten null streams for the four detectors as $\Pi^{aSVW} S_a, \dots, \Pi^{aW+\times} S_a$. This type of null streams including Eq. (3) are discussed by Chatziioannou et al. [21].

If the coefficient of h_V in Eq. (3) vanishes in a certain sky region, there remains only the spin-0 part in the null stream. Thereby, the spin-0 polarization test is possible, if a GW source is found in this sky region. The vanishing coefficient condition is

$$\varepsilon^{abcd} F_a^V F_b^W F_c^+ F_d^\times = 0. \quad (4)$$

This is rewritten in the form of the determinant of a 4×4 matrix as

$$\begin{aligned} D_4 &\equiv \begin{vmatrix} F_1^V & F_1^W & F_1^+ & F_1^\times \\ F_2^V & F_2^W & F_2^+ & F_2^\times \\ F_3^V & F_3^W & F_3^+ & F_3^\times \\ F_4^V & F_4^W & F_4^+ & F_4^\times \end{vmatrix} \\ &= 0. \end{aligned} \quad (5)$$

The components of h_V , h_W , h_+ and h_\times are dependent on a choice of a reference axis in the transverse plane, corresponding to a degree of freedom for a rotation around the GW propagation axis. Therefore, one may ask whether the above condition by Eq. (4) is invariant under the rotational transformation.

We study a rotational transformation of the GW components [18], where the rotation is considered around the GW propagation axis with the rotation angle denoted as η . h_+ and h_\times are spin 2. They are transformed as

$$\begin{pmatrix} \bar{h}_+ \\ \bar{h}_\times \end{pmatrix} = \begin{pmatrix} \cos 2\eta & \sin 2\eta \\ -\sin 2\eta & \cos 2\eta \end{pmatrix} \begin{pmatrix} h_+ \\ h_\times \end{pmatrix}. \quad (6)$$

The bar denotes a quantity after the rotational transformation.

The antenna pattern functions of each detector for h_+ and h_\times are transformed as

$$\begin{pmatrix} \bar{F}_a^+ \\ \bar{F}_a^\times \end{pmatrix} = \begin{pmatrix} \cos 2\eta & -\sin 2\eta \\ \sin 2\eta & \cos 2\eta \end{pmatrix} \begin{pmatrix} F_a^+ \\ F_a^\times \end{pmatrix}. \quad (7)$$

Next, we consider spin 1. h_V and h_W are transformed as

$$\begin{pmatrix} \bar{h}_V \\ \bar{h}_W \end{pmatrix} = \begin{pmatrix} \cos \eta & \sin \eta \\ -\sin \eta & \cos \eta \end{pmatrix} \begin{pmatrix} h_V \\ h_W \end{pmatrix}. \quad (8)$$

The antenna pattern functions of each detector for h_V and h_W are transformed as

$$\begin{pmatrix} \bar{F}_a^V \\ \bar{F}_a^W \end{pmatrix} = \begin{pmatrix} \cos \eta & -\sin \eta \\ \sin \eta & \cos \eta \end{pmatrix} \begin{pmatrix} F_a^V \\ F_a^W \end{pmatrix}. \quad (9)$$

By using Eq. (7), one can show

$$\begin{aligned}\varepsilon^{abcd}\bar{F}_c^+\bar{F}_d^\times &= \varepsilon^{abcd}(F_c^+\cos 2\eta - F_c^\times\sin 2\eta) \\ &\quad \times (F_d^+\sin 2\eta + F_d^\times\cos 2\eta) \\ &= \varepsilon^{abcd}F_c^+F_d^\times,\end{aligned}\quad (10)$$

where ε^{abcd} is a constant for the rotation. Therefore, $\varepsilon^{abcd}F_c^+F_d^\times$ is invariant for the rotational transformation. By using Eq. (9) in the similar manner, we find

$$\begin{aligned}\varepsilon^{abcd}\bar{F}_c^V\bar{F}_d^W &= \varepsilon^{abcd}(F_c^V\cos \eta - F_c^W\sin \eta) \\ &\quad \times (F_d^V\sin \eta + F_d^W\cos \eta) \\ &= \varepsilon^{abcd}F_c^VF_d^W.\end{aligned}\quad (11)$$

Therefore, $\varepsilon^{abcd}F_c^VF_d^W$ is invariant for the rotational transformation.

By combining Eqs. (10) and (11), one can show

$$\varepsilon^{abcd}\bar{F}_a^V\bar{F}_b^W\bar{F}_c^+\bar{F}_d^\times = \varepsilon^{abcd}F_a^VF_b^WF_c^+F_d^\times \quad (12)$$

Therefore, D_4 in Eq. (5) is invariant for the rotation around the GW propagation axis.

Eq. (4), which is equivalent to Eq. (5), describes particular sky positions, in which every of the spin-1 (h^V and h^W) and spin-2 (h^+ and h^\times) parts are eliminated in the null stream. Namely, Eq. (3) for such a particular source location becomes

$$\Pi^{aW+\times}S_a = (\varepsilon^{abcd}F_a^SF_b^WF_c^+F_d^\times)(h_S - h_L) + \Pi^{aW+\times}n_a. \quad (13)$$

A direct test of the scalar modes becomes possible, if the GW source position satisfies Eq. (5). This is a main result of this paper. See Figure 1 for sky locations of $D_4 = 0$. See also Figure 2 for a contour map of D_4 in the sky.

The fraction of sky area for $0.01 \leq |D_4| < 0.1$ (corresponding to the blue region of Figure 2) is 0.37, which means that the probability of a GW event in a finite range $0.01 \leq |D_4| < 0.1$ is 37 percents. But a test of scalar polarizations for this case is very weak. For a stronger test, $|D_4|$ must be smaller. The fraction of sky area for $|D_4| < 0.01$ (covered in the red region of Figure 2) is 0.04. Namely, only four percents of GW170817-like events satisfy this finite range as $|D_4| < 0.01$, which will allow for a stronger direct test of scalar polarizations.

B. Comparison with a *three-detector* null stream approach

For a comparison, we follow References [14, 16] to prepare two sets of detectors for four detectors; the set (1) is the detectors $a = 1, 2, 3$ and the other set (2) is $a = 2, 3, 4$. We define three-dimensional vectors from antenna pattern functions as

$$\vec{F}_{(1)}^I \equiv (F_1^I, F_2^I, F_3^I), \quad (14)$$

$$\vec{F}_{(2)}^I \equiv (F_2^I, F_3^I, F_4^I). \quad (15)$$

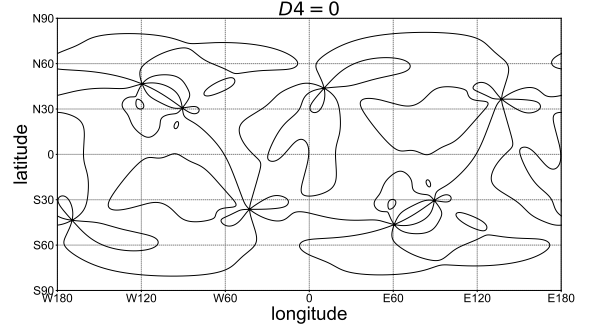


FIG. 1. Sky locations for $D_4 = 0$. We assume aLIGO, Virgo and KAGRA. The vertical axis denotes the latitude and the horizontal axis denotes the longitude, where the coordinate system is earth-centered. Note that this plot does not depend on choices of a polarization angle.

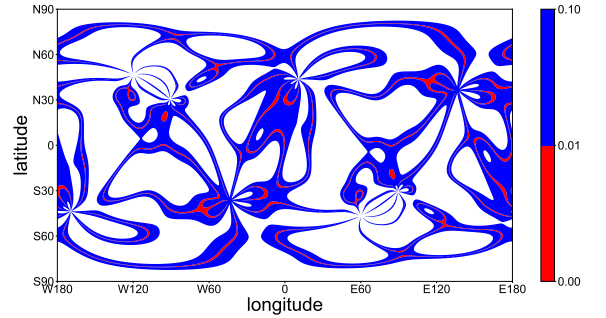


FIG. 2. Contour map of D_4 corresponding to Figure 1. The red and blue (in color) regions denote $0 \leq |D_4| < 0.01$ and $0.01 \leq |D_4| < 0.1$, respectively. Roughly speaking, $|D_4|$ is likely to be $\sim O(1)$, because $|F_a^I| \sim O(1)$. The area for significantly small D_4 such as $0 \leq |D_4| < 0.01$ (red in color) is slight but not negligible in this figure.

We define also vectors for strain outputs and noises as

$$\vec{S}_{(1)} \equiv (S_1, S_2, S_3), \quad (16)$$

$$\vec{S}_{(2)} \equiv (S_2, S_3, S_4). \quad (17)$$

$$\vec{n}_{(1)} \equiv (n_1, n_2, n_3), \quad (18)$$

$$\vec{n}_{(2)} \equiv (n_2, n_3, n_4). \quad (19)$$

The outer product as $\vec{F}_{(1)}^+ \times \vec{F}_{(1)}^\times$ is perpendicular to both $\vec{F}_{(1)}^+$ and $\vec{F}_{(1)}^\times$, where the outer product is defined in a detector space. Therefore, we use it to eliminate the

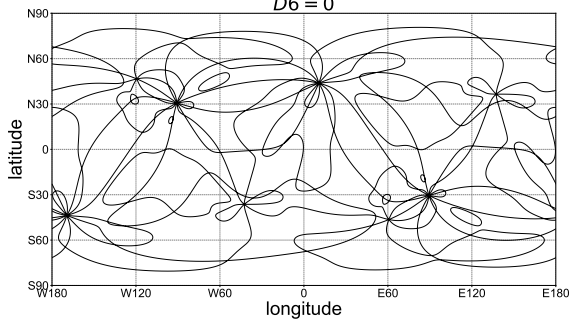


FIG. 3. Plot for $D_6 = 0$, corresponding to Figure 1. The vertical axis denotes the latitude and the horizontal axis denotes the longitude.

spin-2 + and \times modes from the strain outputs.

$$\begin{aligned}
 (\vec{F}_{(1)}^+ \times \vec{F}_{(1)}^\times) \cdot \vec{S}_{(1)} = & [(\vec{F}_{(1)}^+ \times \vec{F}_{(1)}^\times) \cdot \vec{F}_{(1)}^S](h_S - h_L) \\
 & + [(\vec{F}_{(1)}^+ \times \vec{F}_{(1)}^\times) \cdot \vec{F}_{(1)}^V]h_V \\
 & + [(\vec{F}_{(1)}^+ \times \vec{F}_{(1)}^\times) \cdot \vec{F}_{(1)}^W]h_W \\
 & + (\vec{F}_{(1)}^+ \times \vec{F}_{(1)}^\times) \cdot \vec{n}_{(1)}, \quad (20)
 \end{aligned}$$

$$\begin{aligned}
 (\vec{F}_{(2)}^+ \times \vec{F}_{(2)}^\times) \cdot \vec{S}_{(2)} = & [(\vec{F}_{(2)}^+ \times \vec{F}_{(2)}^\times) \cdot \vec{F}_{(2)}^S](h_S - h_L) \\
 & + [(\vec{F}_{(2)}^+ \times \vec{F}_{(2)}^\times) \cdot \vec{F}_{(2)}^V]h_V \\
 & + [(\vec{F}_{(2)}^+ \times \vec{F}_{(2)}^\times) \cdot \vec{F}_{(2)}^W]h_W \\
 & + (\vec{F}_{(2)}^+ \times \vec{F}_{(2)}^\times) \cdot \vec{n}_{(2)}, \quad (21)
 \end{aligned}$$

where \cdot denotes the inner product. These equations are often called null streams in the literature [21–24]. We refer to them as *tensor* null streams, because only the spin-2 modes are completely killed. Tensor null streams are originally for three detectors [20].

If and only if the antenna pattern functions satisfy

$$\begin{aligned}
 D_6^{+\times} \equiv & [(\vec{F}_{(1)}^+ \times \vec{F}_{(1)}^\times) \cdot \vec{F}_{(1)}^V][(\vec{F}_{(2)}^+ \times \vec{F}_{(2)}^\times) \cdot \vec{F}_{(2)}^W] \\
 & - [(\vec{F}_{(1)}^+ \times \vec{F}_{(1)}^\times) \cdot \vec{F}_{(1)}^W][(\vec{F}_{(2)}^+ \times \vec{F}_{(2)}^\times) \cdot \vec{F}_{(2)}^V] \\
 = & 0, \quad (22)
 \end{aligned}$$

$[(\vec{F}_{(1)}^+ \times \vec{F}_{(1)}^\times) \cdot \vec{F}_{(1)}^V]h_V + [(\vec{F}_{(1)}^+ \times \vec{F}_{(1)}^\times) \cdot \vec{F}_{(1)}^W]h_W$ in the right-hand side of Eq. (20) is always proportional to $[(\vec{F}_{(2)}^+ \times \vec{F}_{(2)}^\times) \cdot \vec{F}_{(2)}^V]h_V + [(\vec{F}_{(2)}^+ \times \vec{F}_{(2)}^\times) \cdot \vec{F}_{(2)}^W]h_W$ in the right-hand side of Eq. (21) for any h_V and h_W . Therefore, there exists a linear combination of Eqs. (20) and (21), such that the spin-1 polarizations also can be eliminated. The resultant combination contains only the spin-0 mode with eliminating the other (spin-1 and spin-2) modes. It seems that this is the same as Eq. (13) which was derived from Eq. (3).

Is Eq. (22) equivalent to Eq. (4)? No. This is because $D_6^{+\times}$ in Eq. (22) is of sixth degree in antenna pattern functions, while D_4 in Eq. (5) is of fourth degree. $D_6^{+\times}$

is factorized as

$$D_6^{+\times} = D_4 D_2^{+\times}, \quad (23)$$

where we define

$$D_2^{+\times} \equiv \begin{vmatrix} F_2^+ & F_2^\times \\ F_3^+ & F_3^\times \end{vmatrix}. \quad (24)$$

If

$$D_2^{+\times} = 0, \quad (25)$$

D_6 vanishes even if $D_4 \neq 0$. $D_2^{+\times} = 0$ is a case that tensor antenna pattern functions of the second and third detectors are degenerate. See Figure 3 for sky locations of $D_6 = 0$. For the case of $D_4 \neq 0$, there remains h^V in the right-hand side of Eq. (3). This means that the case of $D_2^{+\times} = 0$ does not lead to a null stream. Therefore, the present formulation to four detectors improves an earlier approach [14, 16] combining two tensor null streams.

Hagihara et al. (2019) considered the two null streams as Eqs. (20) and (21) [16]. They examined whether the four coefficients of h_V or h_W can simultaneously vanish. However, vanishing of the four coefficients is too strong. For a direct test of the scalar modes, it is enough that two coefficients vanish.

C. Adding a fifth detector

Planned LIGO-India is a fifth detector [25]. One of the largest merits of LIGO-India (labeled as $a=I$) comes from its geographic factor, namely being very distant from the other detectors HLVK. LIGO-H and LIGO-L detectors are approximately aligned. Therefore, adding LIGO India is expected to help break some degeneracy between H and L.

By constructing a four-detector null stream including LIGO-India instead of H, we compute D_4 for LVKI. The LIGO-India detector is under planning. The detailed information on the detector is not currently open to public. Therefore, when computing the antenna pattern function of the LIGO-India detector, the coordinates of the LIGO-India detector are approximated by those of the Hingoli city (19.72°N, 77.15°E) [25] and we assume that the detector arms are aligned to the east and north directions, respectively, for its simplicity. See Figure 4 for a contour map of D_4 for LVKI.

The areas covered in the red and blue (in color) region in Figure 4 are comparable to those in Figure 2 for HLVK. The sky fraction of the red region ($|D_4| < 0.01$) in Figure 4 is 0.03. The fraction of the blue region ($0.01 \leq |D_4| < 0.1$) is 0.33. In Figure 2, they are 0.04 and 0.37, respectively. We consider also different sets of detectors to evaluate D_4 . See Table I.

We consider two different arm directions by 30-degree rotation from the east direction and 45-degree rotation (namely north-east direction). See Table II.

TABLE I. Area fraction in the sky for $|D_4| < 0.01$ and $0.01 \leq |D_4| < 0.1$. We consider five sets of HLVK, LVKI, HVKI, HLKI and HLVI.

	$ D_4 < 0.01$	$0.01 \leq D_4 < 0.1$
HLVK	0.04	0.37
LVKI	0.03	0.33
HVKI	0.03	0.33
HLKI	0.05	0.43
HLVI	0.04	0.37

TABLE II. Area fraction in the sky for $|D_4| < 0.01$ and $0.01 \leq |D_4| < 0.1$. We consider three cases of the arm directions for LVKI.

	$ D_4 < 0.01$	$0.01 \leq D_4 < 0.1$
LVKI 0° (East)	0.03	0.33
LVKI 30°	0.04	0.35
LVKI 45° (North-east)	0.04	0.32

These calculations show that replacing one of HLVK by LIGO-India in a four-detector null stream does not so much affect the area fraction. Namely, the area fraction is almost independent of a choice of a detector set in the four-detector null stream. But adding LIGO-India gives us four more sets of four-detector null streams. Roughly speaking, therefore, the total area fraction for HLVKI becomes five-times larger than only the HLVK network.

Furthermore, we should stress that Eq. (1) for strain outputs ($a = 1, \dots, 5$) from the five detectors including LIGO-India can be always solved for the five modes $h_S - h_L, h_V, h_W, h_+$ and h_\times . This means that, in principle, adding LIGO-India will allow for a direct test of each GW polarization for *any* sky region. This would be an important step in testing our gravitational theories.

III. ON THE ARRIVAL TIME OF EXTRA POLARIZATION MODES

In discussions from Eq. (6) to Eq. (13), we assume that the speeds of the same spin modes are identical. But a different spin mode may travel at different speed. We denote the speed of spin- h mode ($h = 0, 1, 2$) as c_h . We examine whether the shift of the arrival time difference from detector to detector should be changed for extra polarization modes.

At the Earth, the arrival time difference between the spin- h mode and the light signal is

$$\delta t_h = \frac{D}{c} - \frac{D}{c_h}, \quad (26)$$

where D is the distance to the source. The arrival time difference between two detectors (a and b) for the spin- h

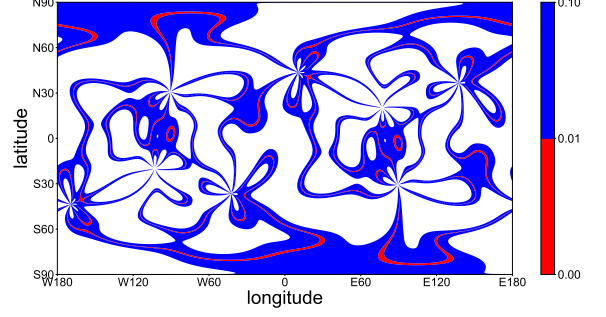


FIG. 4. Contour map of D_4 for LVKI network, corresponding to Figure 2 for HLVK. The coordinates of the LIGO-India detector are approximated by those of the Hingoli city (19.72°N , 77.15°E) [25] and we assume that the detector arms are aligned to the east and north directions, respectively, for its simplicity. The red and blue (in color) regions denote $0 \leq |D_4| < 0.01$ and $0.01 \leq |D_4| < 0.1$, respectively.

mode is defined as

$$\Delta t_{ab} \equiv \frac{D_a - D_b}{c_h}, \quad (27)$$

where D_a and D_b denote the distance from the source to the detector a and b , respectively. By combining Eqs. (26) and (27), we eliminate c_h to obtain

$$\Delta t_{ab} = \frac{D_a - D_b}{c} - \frac{D_a - D_b}{D} \delta t_h. \quad (28)$$

The first term in the right-hand side of Eq. (28) is the normal arrival time difference between detectors, which has been already taken into account in the GW data analysis. The second term is due to the deviation from the light speed. The arrival time difference between detectors by $c_h - c$ is roughly estimated as

$$\left| \frac{D_a - D_b}{D} \delta t_h \right| \sim 2 \times 10^{-14} \text{sec.} \times \left(\frac{|D_a - D_b|}{6 \times 10^3 \text{km}} \right) \left(\frac{40 \text{Mpc}}{D} \right) \left(\frac{|\delta t_h|}{3600 \text{sec.}} \right). \quad (29)$$

We assume $|D_a - D_b| \sim$ the Earth size and the data analysis duration for one GW event is ~ 3600 seconds for the simplicity. If the extra mode arrives much later, say a few weeks later, we can hardly recognize that it came from the same event. A few-hours delay may be identified as the same event in data analysis. Therefore, a case that a hypothetical scalar is nearly massless can be tested in the present approach, while a scalar with heavy mass is beyond the reach of the present method because of large delay. If we analyze the data for testing extra modes arriving before an hour later, the correction to the arrival time difference between detectors for $D \sim 40 \text{Mpc}$ is around $\sim 10^{-14}$ seconds, which may be currently negligible in the data analysis of waves with the frequency band around a few kHz.

IV. CONCLUSION

We considered strain outputs at four noncoaligned detectors such as a network of aLIGO-Hanford, aLIGO-Livingston, Virgo and KAGRA [13]. Generally speaking, five unknowns $\{h_S - h_L, h_V, h_W, h_+, h_\times\}$ cannot be determined from four outputs $\{S_1, S_2, S_3, S_4\}$. If a sky location of a GW source with the EM counterpart satisfies a single equation that we proposed in this paper, both the spin-1 modes and spin-2 ones can be eliminated from a certain combination of strain outputs at the four detectors, where this equation describes curves on the celestial sphere. If a GW source is found in the curve (or its neighborhood practically), a direct test of the scalar modes separately from the other (vector and tensor) modes becomes possible in principle. The possibility of such a direct test is higher than the earlier expectation (Hagihara et al. PRD, 100, 064010, 2019), which argued that the vector modes could not be completely eliminated. We

discussed also that adding the planned LIGO-India detector as a fifth detector would significantly increase the feasibility of scalar polarization tests. Detailed numerical simulations with using binary models will be left for future work.

ACKNOWLEDGMENTS

We would like to thank Atsushi Nishizawa for useful discussions. We would like to thank Hideyuki Tagoshi and Jishnu Suresh for the information on the current status of the planned LIGO-India detector. We wish to thank Seiji Kawamura, Kipp Cannon, Nobuyuki Kanda, and Yousuke Itoh for stimulating conversations. We thank Yuuiti Sendouda and Toshiaki Ono for the useful conversations. H. A. is supported in part by Japan Society for the Promotion of Science (JSPS) Grant-in-Aid for Scientific Research, No. 17K05431, and in part by Ministry of Education, Culture, Sports, Science, and Technology, No. 17H06359.

-
- [1] A. Einstein, Sitzungsber. Preuss. Akad. Wiss. Berlin (Math. Phys.) **1916**, 688 (1916).
 - [2] A. Einstein, Sitzungsber. Preuss. Akad. Wiss. Berlin (Math. Phys.) **1918**, 154 (1918).
 - [3] C. M. Will, Living Rev. Relativity, **17**, 4 (2014).
 - [4] D. M. Eardley, D. L. Lee, A. P. Lightman, R. V. Wagoner, and C. M. Will, Phys. Rev. Lett. **30**, 884 (1973).
 - [5] A. Nishizawa, A. Taruya, K. Hayama, S. Kawamura, and M. A. Sakagami, Phys. Rev. D **79**, 082002 (2009).
 - [6] B. P. Abbott et al. (Virgo and LIGO Scientific Collaborations), Phys. Rev. Lett. **116**, 221101 (2016).
 - [7] B. P. Abbott et al. (Virgo and LIGO Scientific Collaborations), Phys. Rev. Lett. **119**, 141101 (2017).
 - [8] B. P. Abbott et al. (Virgo and LIGO Scientific Collaborations), Phys. Rev. Lett. **123**, 011102 (2019).
 - [9] K. Hayama, and A. Nishizawa, Phys. Rev. D **87**, 062003 (2013).
 - [10] M. Isi, A. J. Weinstein, C. Mead, and M. Pitkin, Phys. Rev. D **91**, 082002 (2015).
 - [11] M. Isi, M. Pitkin, and A. J. Weinstein, Phys. Rev. D **96**, 042001 (2017).
 - [12] H. Takeda, A. Nishizawa, Y. Michimura, K. Nagano, K. Komori, M. Ando, and K. Hayama, Phys. Rev. D **98**, 022008 (2018).
 - [13] B. P. Abbott, Living. Rev. Relativ., **21**, 3 (2018).
 - [14] Y. Hagihara, N. Era, D. Iikawa, and H. Asada, Phys. Rev. D **98**, 064035 (2018).
 - [15] Y. Fujii, and K. Maeda, *Scalar-Tensor Theory of Gravitation*, (Cambridge Univ. Press, UK. 2008).
 - [16] Y. Hagihara, N. Era, D. Iikawa, A. Nishizawa, and H. Asada, Phys. Rev. D **100**, 064010 (2019).
 - [17] B. P. Abbott, et al., Astrophys. J. Lett. **848**, L12 (2017); B. P. Abbott, et al., Astrophys. J. Lett. **848**, L13 (2017).
 - [18] E. Poisson, and C. M. Will, *Gravity*, (Cambridge Univ. Press, UK. 2014).
 - [19] The present paper follows Chapter 13 in Poisson and Will [18] to define the GW antenna patterns. See Nishizawa et al. [5] and also a pioneering work for purely TT waves by Schutz and Tinto [20]. Note that their definitions are a little different from each other [5, 18].
 - [20] B. F. Schutz, and M. Tinto, Mon. Not. R. Astr. Soc. **224**, 131 (1987).
 - [21] K. Chatziioannou, N. Yunes, and N. Cornish, Phys. Rev. D **86**, 022004 (2012).
 - [22] Y. Gürsel, and M. Tinto, Phys. Rev. D **40**, 3884 (1989).
 - [23] L. Wen, and B. F. Schutz, Class. Quant. Grav. **22**, S1321 (2005).
 - [24] S. Chatterji, A. Lazzarini, L. Stein, P. J. Sutton, A. Searle, and M. Tinto, Phys. Rev. D **74**, 082005 (2006).
 - [25] <http://www.ligo-india.in/environmental-clearance-given-to-ligo-india/>